

# Impedance Synthesis of Plane Diffraction Vibrator Arrays

Yuriy M. Penkin, Victor A. Katrich, Mikhail V. Nesterenko\*,  
Sergey L. Berdnik, and Svetlana V. Pshenichnaya

**Abstract**—The problem of impedance synthesis of two-dimensional diffraction arrays of thin linear vibrators, whose geometric centers are located at the nodes of a flat rectangular grid with double periodicity is solved analytically. The problem is formulated as follows: the complex surface impedances of the vibrators should be determined which allows to steer the diffraction radiation maximum of the array to any predefined direction. The problem is solved under following assumptions: array is excited by a polarized plane wave, and the radiation pattern (RP) of each vibrator element in the array coincides with that of an isolated radiator. The correctness of the solution is verified by simulations using the formulas for the vibrator impedances for the 5 by 5 antenna array.

## 1. INTRODUCTION

The main advantage of antenna arrays is related to electric scanning of its radiation pattern [1–3]. The scanning can be continuous or discrete, depending on a control signal mode. Antenna arrays working in a discrete-switching mode are called step scanning antennas. The scanning antennas array can also be classified by an excitation mode of their elements. The analysis of antenna arrays with spatial excitation of an optical type known as diffraction array is still important for modern practice.

Of course, the diffraction arrays with discrete-switching can be implemented by using different types of elements, including impedance vibrators. In this case, there exists a possibility to use a surface impedance of vibrator elements as additional factor to control the array RP by varying electrical lengths of the vibrators and, therefore, the amplitude-phase distribution over the array aperture [4, 5]. From these positions, the authors studied the one-dimensional antenna dipole array in [6], where the application of impedance synthesis for controlling scanning angles of the array RP maximum was justified. Moreover, the problem of an equidistant linear antenna array with symmetric vibrator excitation by delta voltage generators was solved analytically. This paper is aimed at generalization of the analytical solution of the impedance synthesis problem to the case of two-dimensional plane of diffraction vibrator arrays. In the first step, to illustrate the analytical approach, we will use the simplified theory of antenna array without taking into account the mutual coupling between array elements [7, 8].

## 2. FORMULATION OF THE IMPEDANCE SYNTHESIS PROBLEM

Let us consider a 2D diffraction array of impedance vibrators shown in Fig. 1. The array is located in infinite medium with material parameters  $(\epsilon_1; \mu_1)$  in the plane  $(x_0z)$  of Cartesian coordinate system  $(x, y, z)$ . The parameters of the diffraction array are:  $N_z$  is the number of rows,  $N_x$  the number of vibrators in a row,  $d_z$  the the distance between adjacent rows, and  $d_x$  the distance vibrators in the row.

*Received 9 August 2019, Accepted 3 January 2020, Scheduled 26 January 2020*

\* Corresponding author: Mikhail V. Nesterenko (mikhail.v.nesterenko@gmail.com).

The authors are with the Department of Radiophysics, Biomedical Electronics and Computer Systems, V. N. Karazin Kharkiv National University, 4, Svobody Sq., Kharkiv 61022, Ukraine.

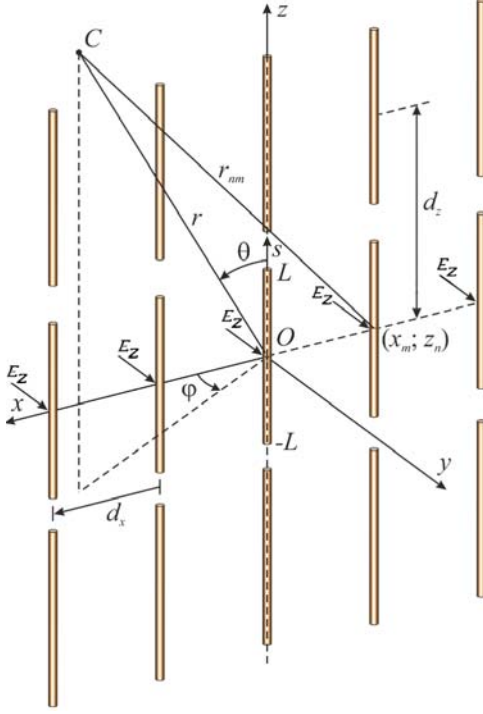


**Figure 1.** The geometry of the diffraction antenna array.

Let us also introduce spherical coordinates  $(r, \theta, \varphi)$ , in which polar axis coincides with the axis  $\{0z\}$ , and angle  $\varphi$  is measured from the axis  $\{0x\}$ .

Without losing generality, we assume that the length of all  $N = N_z \times N_x$  vibrators is  $2L$  (rather than  $dz > 2L$ ), and the radius  $\rho_{nm}$  of the vibrator with indices  $nm$  ( $n \in [1, N_x]$ ,  $m \in [1, N_y]$ ) satisfies the thin-wire approximation  $\frac{\rho_{nm}}{2L} \ll 1$ ,  $\frac{\rho_{nm}\sqrt{\varepsilon_1\mu_1}}{\lambda} \ll 1$  ( $\lambda$  is the free space wavelength). Each vibrator is characterized by the constant impedance  $\bar{Z}_{nm}$  normalized to the medium wave impedance  $Z_0 = \sqrt{\mu_1/\varepsilon_1}\Omega$ . Let us consider an array excitation by a monochromatic plane polarized wave  $E_z = E_0 e^{ik_1 y}$  ( $k_1 = k\sqrt{\varepsilon_1\mu_1}$ ,  $k = \omega/c$  are wave numbers, and  $c \approx 2.998 \cdot 10^{10}$  cm/s) incident normally on the array from a half-space  $y \leq 0$ . If temporal dependence is given in the form  $e^{i\omega t}$  where  $t$  is the time,  $\omega$  is the circular frequency, and the longitudinal electric currents  $J_{nm}(s)$  on the vibrator elements can be represented by the zero approximation relative to the first degree of a natural small parameter  $\alpha$  [5]

$$J_{nm}(s) = -\alpha_{nm} \frac{i\omega}{k_1 \tilde{k}_{nm}} E_0 \frac{\cos \tilde{k}_{nm}s - \cos \tilde{k}_{nm}L}{\cos \tilde{k}_{nm}L + \alpha_{nm} P^s[k_1 \rho_{nm}, k_1 L]}, \quad (1)$$

where

$$P^s(k_1 \rho_{nm}, k_1 L) = \cos k_1 L [2 \ln 2 - \gamma_{nm}(L) - (1/2) \text{Cin}(2k_1 L) - (i/2) \text{Si}(4k_1 L)] + \sin k_1 L [(1/2) \text{Si}(4k_1 L) - (i/2) \text{Cin}(4k_1 L)],$$

$\tilde{k}_{nm}^2(s) = k_1^2 \left(1 + \frac{i2\alpha_{nm}}{k_1 \rho_{nm}} \bar{Z}_{nm}\right) = k_1^2 \left(1 + i2\alpha_{nm} \bar{\beta}_{nm}\right)$  are coefficients;  $\alpha_{nm} = \frac{1}{2 \ln[\rho_{nm}/(2L)]}$  are the natural small parameters;  $\bar{\beta}_{nm} = \frac{\bar{Z}_{nm}}{k_1 \rho_{nm}}$ ;  $\gamma_{nm}(L) = \ln \frac{\rho_{nm}[2L + \sqrt{4L^2 + \rho_{nm}^2}]}{4L^2}$ ;  $\text{Si}(x)$  and  $\text{Cin}(x)$  are sine and cosine integrals of the complex argument, and

$$\begin{aligned} \alpha_{nm} \int_{-L}^L \frac{e^{-ik_1 \sqrt{(L-s)^2 + \rho_{nm}^2}}}{\sqrt{(L-s)^2 + \rho_{nm}^2}} \cos \tilde{k}_{nm}s ds &\approx \alpha_{nm} \int_{-L}^L \frac{e^{-ik_1 \sqrt{(L-s)^2 + \rho_{nm}^2}}}{\sqrt{(L-s)^2 + \rho_{nm}^2}} \\ &[\cos(k_1 s) - ik_1 L s \alpha_{nm} \bar{\beta}_{nm} \sin(k_1 s)] ds \approx \alpha_{nm} \int_{-L}^L \frac{e^{-ik_1 \sqrt{(L-s)^2 + \rho_{nm}^2}}}{\sqrt{(L-s)^2 + \rho_{nm}^2}} \cos(k_1 s) ds. \end{aligned}$$

Then the main component of the wave zone electric field reradiated by the vibrator can be written as

$$E_{nm}^\theta = \frac{60\pi i}{\lambda} \cdot \frac{e^{-ik_1 r_{nm}}}{r_{nm}} \sin \theta \int_{-L}^L J_{nm}(s) e^{isk_1 \cos \theta} ds = 120\pi \frac{e^{-ik_1 r_{nm}}}{\lambda k_1^2 r_{nm}} \cdot \frac{1}{\cos \theta} \cdot \frac{\alpha_{nm} \omega E_0 \sin \theta}{\tilde{k}_{nm}^2 - k_1^2 \cos^2 \theta} \\ \times \frac{k_1 \cos \theta \sin(\tilde{k}_{nm} L) \cos(k_1 L \cos \theta) - \tilde{k}_{nm} \cos(\tilde{k}_{nm} L) \sin(k_1 L \cos \theta)}{\cos \tilde{k}_{nm} L + \alpha_{nm} P^s[k_1 \rho_{nm}, k_1 L]}. \quad (2)$$

The components  $E_\varphi$  and  $E_r$  of the electric field diffracted at single vibrator in the coordinate system  $(r, \theta, \varphi)$  are equal to zero. If phases of fields arriving at the observation point  $C(r, \theta, \varphi)$  are taken into account, the total wave zone reradiation field of the diffraction array  $E_\theta(r, \theta, \varphi)$  is equal to the sum of the secondary radiation fields of each vibrator. Therefore, we can write

$$E_\theta(r, \theta, \varphi) = \frac{120\pi \omega E_0 \sin \theta}{\lambda k_1^2 \cos \theta} \sum_{n=1}^{N_z} \sum_{m=1}^{N_x} \frac{e^{-ik_1 r_{nm}}}{r_{nm}} \cdot \frac{\alpha_{nm}}{\tilde{k}_{nm}^2 - k_1^2 \cos^2 \theta} \\ \times \frac{k_1 \cos \theta \sin(\tilde{k}_{nm} L) \cos(k_1 L \cos \theta) - \tilde{k}_{nm} \cos(\tilde{k}_{nm} L) \sin(k_1 L \cos \theta)}{\cos \tilde{k}_{nm} L + \alpha_{nm} P^s[k_1 \rho_{nm}, k_1 L]}. \quad (3)$$

The impedance synthesis problem can be formulated as follows: for a given direction  $(\theta_{\max}, \varphi_{\max})$  of the maximum of the secondary radiation field in the wave zone, the impedances  $\bar{Z}_{nm}$  of each vibrator element can be determined based on Equation (3).

### 3. SOLUTION OF THE IMPEDANCE SYNTHESIS PROBLEM

First, let us convert Equation (2) defining the field of secondary field reradiated by an isolated vibrator [6] taking into account the relations  $\tilde{k}_{nm} \approx k_1 (1 + i\alpha_{nm} \bar{\beta}_{nm})$  and  $\tilde{k}_{nm}^2 - k_1^2 \cos^2 \theta = k_1^2 (\sin^2 \theta + 2i\alpha_{nm} \bar{\beta}_{nm})$  valid due to the smallness of the parameter  $\alpha$ , and representations of trigonometric functions  $\sin(\tilde{k}_{mn} L) \approx \sin(k_1 L) + ik_1 L \alpha_{mm} \bar{\beta}_{mm} \cos(k_1 L)$  and  $\cos(\tilde{k}_{mn} L) \approx \cos(k_1 L) - ik_1 L \alpha_{mn} \bar{\beta}_{nm} \sin(k_1 L)$  valid up to terms of  $\alpha^2$ . Then we can write

$$E_{nm}^\theta = 120\pi \frac{e^{-ik_1 r_{nm}}}{\lambda k_1^3 r_{nm}} \cdot \frac{\alpha_{nm} \omega E_0}{\cos \theta \sin^3 \theta} (f_1(\theta) \sin^2 \theta + i\alpha_{nm} \bar{\beta}_{nm} [f_2(\theta) \sin^2 \theta - 2f_1(\theta)]), \quad (4a)$$

where

$$f_1(\theta) = \frac{\cos \theta \sin(k_1 L) \cos(k_1 L \cos \theta) - \cos(k_1 L) \sin(k_1 L \cos \theta)}{\cos \tilde{k}_{nm} L + \alpha_{nm} P^s[k_1 \rho_{nm}, k_1 L]}, \\ f_2(\theta) = \frac{k_1 L \cos \theta \cos(k_1 L) \cos(k_1 L \cos \theta) + \sin(k_1 L \cos \theta) [k_1 L \sin(k_1 L) - \cos(k_1 L)]}{\cos \tilde{k}_{nm} L + \alpha_{nm} P^s[k_1 \rho_{nm}, k_1 L]}.$$

After defining

$$C_{nm} = \cos(k_1 L) + \alpha_{nm} \operatorname{Re}(P^s[k_1 \rho_{nm}, k_1 L]),$$

$$\tilde{f}_1(\theta) = \cos \theta \sin(k_1 L) \cos(k_1 L \cos \theta) - \cos(k_1 L) \sin(k_1 L \cos \theta),$$

$$\tilde{f}_2(\theta) = k_1 L \cos \theta \cos(k_1 L) \cos(k_1 L \cos \theta) + \sin(k_1 L \cos \theta) [k_1 L \sin(k_1 L) - \cos(k_1 L)]$$

the expression for  $E_{nm}^\theta$  can be written as

$$E_{nm}^\theta = 120\pi \frac{e^{-ik_1 r_{nm}}}{\lambda k_1^3 r_{nm}} \cdot \frac{\alpha_{nm} \omega E_0}{C_{nm} \cos \theta \sin \theta} \left\{ \begin{array}{l} \tilde{f}_1(\theta) - i\alpha_{nm} \frac{\tilde{f}_1(\theta)}{C_{nm}} \operatorname{Im}(P^s[k_1 \rho_{nm}, k_1 L]) \\ + i\alpha_{nm} \bar{\beta}_{nm} \left[ \frac{\tilde{f}_2(\theta) \sin^2 \theta - 2\tilde{f}_1(\theta)}{\sin^2 \theta} + \frac{\tilde{f}_1(\theta)}{C_{nm}} k_1 L \sin(k_1 L) \right] \end{array} \right\}. \quad (4b)$$

Equation (4b) is more convenient for the analysis, since the first two terms in curly bracket determine the RP of the isolated perfectly conducting vibrator, while the third term defines the field variation due to the impedance coating of the vibrator.

If the difference of geometric path for the waves propagating from neighboring vibrators and observation point  $C(r, \theta, \varphi)$  is taken into account, the expression for the total secondary radiation field in the wave zone can be presented based on Eq. (4b) as follows [4, 7, 8]

$$E_\theta(\theta, \varphi) = \frac{120\pi\omega E_0}{k_1^3 \lambda \cos \theta \sin \theta} e^{-i(N_z+1)u/2} e^{-i(N_x+1)v/2} \sum_{n=1}^{N_z} \sum_{m=1}^{N_x} \frac{\alpha_{nm}}{C_{nm}} e^{i(nu+mv)} \times \left\{ \begin{array}{l} \tilde{f}_1(\theta) - i\alpha_{nm} \frac{\tilde{f}_1(\theta)}{C_{nm}} \text{Im}(P^s[k_1\rho_{nm}, k_1L]) \\ + i\alpha_{nm} \bar{\beta}_{nm} \left[ \frac{\tilde{f}_2(\theta) \sin^2 \theta - 2\tilde{f}_1(\theta)}{\sin^2 \theta} + \frac{\tilde{f}_1(\theta)}{C_{nm}} k_1 L \sin(k_1 L) \right] \end{array} \right\} \quad (5)$$

where  $u = k_1 d_z \cos \theta$  and  $v = k_1 d_x \sin \theta \cos \varphi$ . If the array vibrators are perfectly conducting,  $\bar{\beta}_{nm} = \bar{Z}_{nm} = 0$ , and amplitudes of all vibrator currents are equal to  $J_{mn} = J_0 = \frac{120\pi\alpha\omega E_0}{Ck_1^3 \lambda} [1 - i\frac{\alpha}{C} \text{Im}(P^s[k_1\rho, k_1L])]$ , then  $\alpha_{nm} = \alpha$ ,  $\rho_{nm} = \rho$ ,  $C = C_{nm}|_{\alpha_{mn}=\alpha, \rho_{nm}=\rho}$  and Equation (5) is reduced to

$$E_\theta(\theta, \varphi) = J_0 e^{-i(N_z+1)u/2} e^{-i(N_x+1)v/2} \frac{\tilde{f}_1(\theta)}{\cos \theta \sin \theta} \sum_{n=1}^{N_z} \sum_{m=1}^{N_x} e^{i(nu+mv)}. \quad (6)$$

As can be seen, the RP maximum is directed along the axis  $\{0y\}$  ( $\theta = \pi/2, \varphi = \pi/2$ ) under condition  $u = v = 0$ . One can also see that the common array factor in Equation (6) is a product of two independent series describing the RP of the two linear vibrator arrays whose axes are directed along axes  $\{0x\}$  and  $\{0z\}$ .

As known from the antenna array theory (for example, [7, 8]), the rotational displacement of the RP in space can be realized by linear phase shifts between the currents of the vibrators. If the phase shift between waves arriving at observation point from adjacent vibrator rows is  $\Delta u$ , and that from adjacent vibrator in a row is  $\Delta v$ , the direction of the antenna array RP maximum  $(\theta_{\max}; \varphi_{\max})$  is determined by the following relations

$$\cos \theta_{\max} = \Delta u / k_1 d_z \quad \text{and} \quad \sin \theta_{\max} \cos \varphi_{\max} = \Delta v / k_1 d_x. \quad (7)$$

Then Equation (6) can be rewritten as

$$E_\theta(\theta, \varphi) = J_0 e^{-i(N_z+1)u/2} e^{-i(N_x+1)v/2} \frac{\tilde{f}_1(\theta)}{\cos \theta \sin \theta} \sum_{n=1}^{N_z} \sum_{m=1}^{N_x} e^{i(nu+mv)} e^{-i[(n-1)\Delta u + (m-1)\Delta v]}. \quad (8)$$

As can be seen from the above formulas, Equations (5) and (8) are identical if the following relations

$$\begin{aligned} & e^{-ik_1[(n-1)d_z \cos \theta + (m-1)d_x \sin \theta \cos \varphi]} - 1 \\ &= i\alpha \bar{\beta}_{nm} \frac{C \tilde{f}_2(\theta) \sin^2 \theta - \tilde{f}_1(\theta) [2C - k_1 L \sin(k_1 L) \sin^2 \theta]}{\tilde{f}_1(\theta) \sin^2 \theta [C - i\alpha \text{Im}(P^s[k_1\rho, k_1L])]} \Big|_{\theta=\theta_{\max}; \varphi=\varphi_{\max}} \end{aligned} \quad (9)$$

are valid for all indices  $n$  and  $m$ . The relations in Eq. (9) can be used as equations allowing to find the unknowns  $\{\bar{\beta}_{nm}\}$  for any angle  $(\theta_{\max}; \varphi_{\max})$ .

Let us denote  $\chi_{nm} = [(n-1)d_z \cos \theta_{\max} + (m-1)d_x \sin \theta_{\max} \cos \varphi_{\max}]$ , as the phase parameter,  $D = \frac{C \tilde{f}_2(\theta) \sin^2 \theta - \tilde{f}_1(\theta) [2C - k_1 L \sin(k_1 L) \sin^2 \theta]}{\tilde{f}_1(\theta) \sin^2 \theta} \Big|_{\theta=\theta_{\max}}$  as the functional multiplier, and  $\bar{Z}_{nm} = \bar{R}_{nm} + i\bar{X}_{nm}$

as the complex impedance, where  $\bar{R}_{nm}$  and  $\bar{X}_{nm}$  are the real and imaginary parts of the impedance. Then Equation (9) can be written in the following form

$$1 - e^{-ik_1 \chi_{nm}} = -i\alpha \frac{\bar{R}_{nm} + i\bar{X}_{nm}}{k_1 \rho} \frac{D}{C - i\alpha \text{Im}(P^s[k_1\rho, k_1L])}. \quad (10)$$

For lossless media, parameter  $\alpha$  is real, and the relations in Equation (10) can be rewritten as

$$\frac{i\alpha D\bar{R}_{nm} - \alpha D\bar{X}_{nm}}{k_1\rho} = -[1 - \cos(k_1\chi_{nm}) + i\sin(k_1\chi_{nm})] \times [C - i\alpha \text{Im}(P^s[k_1\rho, k_1L])]. \quad (11)$$

Substituting  $C$  defined in the relations of Equation (4a) into Equation (11), we obtain the identity

$$\begin{aligned} & \frac{i\alpha D\bar{R}_{nm} - \alpha D\bar{X}_{nm}}{k_1\rho} - [1 - \cos(k_1\chi_{nm})] \\ & \times [\cos(k_1L) + \alpha \text{Re}(P^s[k_1\rho, k_1L]) - \alpha \sin(k_1\chi_{nm}) \text{Im}(P^s[k_1\rho, k_1L])] \\ & - i\sin(k_1\chi_{nm}) [\cos(k_1L) + \alpha \text{Re}(P^s[k_1\rho, k_1L])] + i\alpha \text{Im}(P^s[k_1\rho, k_1L]) [1 - \cos(k_1\chi_{nm})], \end{aligned} \quad (12)$$

Denoting the real and imaginary parts of the functional  $P^s[k_1\rho_{nm}, k_1L]$  defined in Eq. (1) as

$$\begin{aligned} \text{Re}(P^s) &= \cos k_1L [2 \ln 2 - \gamma_{nm}(L) - (1/2)\text{Cin}(2k_1L)] + (1/2)\text{Si}(4k_1L) \sin k_1L, \\ \text{Im}(P^s) &= -(1/2) [\text{Si}(4k_1L) \cos k_1L + \text{Cin}(4k_1L) \sin k_1L], \end{aligned} \quad (13)$$

we can represent the relation of Equation (12) in the form

$$\begin{aligned} \frac{i\alpha D\bar{R}_{nm} - \alpha D\bar{X}_{nm}}{k_1\rho} &= -[1 - \cos(k_1\chi_{nm})] \times [\cos(k_1L) + \alpha \text{Re}(P^s)] - \alpha \sin(k_1\chi_{nm}) \text{Im}(P^s) \\ & - i\sin(k_1\chi_{nm}) [\cos(k_1L) + \alpha \text{Re}(P^s)] + i\alpha \text{Im}(P^s) [1 - \cos(k_1\chi_{nm})], \end{aligned} \quad (14)$$

The final formulas for the real and imaginary parts of the surface impedance of the array vibrators can be obtained based on Eq. (14), as

$$\begin{aligned} \bar{R}_{nm} &= \frac{k_1\rho}{\alpha D} \left\{ \begin{array}{l} \alpha \text{Im}(P^s) [1 - \cos(k_1\chi_{nm})] \\ - \sin(k_1\chi_{nm}) [\cos(k_1L) + \alpha \text{Re}(P^s)] \end{array} \right\}, \\ \bar{X}_{nm} &= \frac{k_1\rho}{\alpha D} \left\{ \begin{array}{l} \alpha \sin(k_1\chi_{nm}) \text{Im}(P^s) \\ + [1 - \cos(k_1\chi_{nm})] \times [\cos(k_1L) + \alpha \text{Re}(P^s)] \end{array} \right\}, \end{aligned} \quad n = 1, 2 \dots N_x; m = 1, 2 \dots N_y. \quad (15)$$

Equations (15) are valid for any number of vibrators in the array and arbitrary distances between the vibrators. However, in the general case, the impedance  $\bar{Z}_{nm} = \bar{R}_{nm} + i\bar{X}_{nm}$  defined as effective physical quantities does not guarantee that the condition  $\bar{R}_{nm} \geq 0$  can be always fulfilled. Since this condition, put forward based on energy laws, determines the possibility of practical realization in the form of vibrator intrinsic impedance, the fulfillment of the condition  $\bar{R}_{Sn} \geq 0$  should always be checked in the course of numerical simulations.

The total field  $E_{\Sigma}^{\theta}(r, \theta, \varphi)$  in the upper half-space above the array can be represented as the sum of the excitation and secondary radiation field, that is, the incident plane wave field and the field diffracted by the antenna array. Therefore, we can write

$$E_{\Sigma}^{\theta}(r, \theta, \varphi) = E_0 e^{-ik_1 r \cos \theta} + \sum_{n=1}^{N_z} \sum_{m=1}^{N_x} E_{nm}^{\theta}, \quad (16)$$

which states that the formation of the antenna RP in the wave zone is determined only by the diffraction component.

#### 4. NUMERICAL RESULTS

The electromagnetic wave incident at an obstacle, whose dimensions are commensurate with the radiation field wavelength in the medium, is scattered in all directions. If the obstacle is characterized by periodic variation of any parameter influencing the wave propagation, its energy is scattered in discrete directions, known as diffraction orders. The main diffraction order in such structures can be analyzed by using scattering matrices which include the energy reflection and transmission coefficients [9]. However, the key stage is still the study of the diffraction characteristics of the structures that are changed due to variation of the vibrator impedance. Therefore, the simulation of the antenna arrays can be carried out based on the diffraction characteristics.

As an example, consider the diffraction array consisting of  $N$  symmetric resonant impedance vibrators ( $N = 25$ ,  $N_x = 5$ ,  $N_z = 5$ ), whose length and radius are  $2L = 0.4908\lambda$  and  $\rho_{nm} = L/75$ . To solve the problem, the impedance of each vibrator should be found based on Equations (15) so that the RP maximum is scanned in the direction defined by the angle  $(\theta_{\max}; \varphi_{\max})$ . When the procedure of impedances synthesis procedure is completed, the array RD should be computed by using Equation (16).

The simulation results are presented for the two impedance arrays with the geometric parameters:  $d_z = 0.5\lambda$ ,  $d_x = 0.5\lambda$  and  $d_z = 0.5\lambda$ ,  $d_x = 0.25\lambda$ . The simulation results are shown as deviations of the angle  $(\theta_{\max}; \varphi_{\max})$  symmetrical relative to the array normal ( $\theta = 90^\circ$ ;  $\varphi = 90^\circ$ ), which corresponds to the direction of the RP maxima of the array with perfectly conducting vibrators.

The cross sections of the normalized array RP plotted, based on Equation (16), as a function of the RP maxima deviation in the plane  $\theta_{\max} = 90^\circ$  are shown in Fig. 2. The plots of the RP as functions of the angular coordinates  $\varphi^\circ$  and  $\theta^\circ$  are shown in Fig. 2(a) and Fig. 2(b).

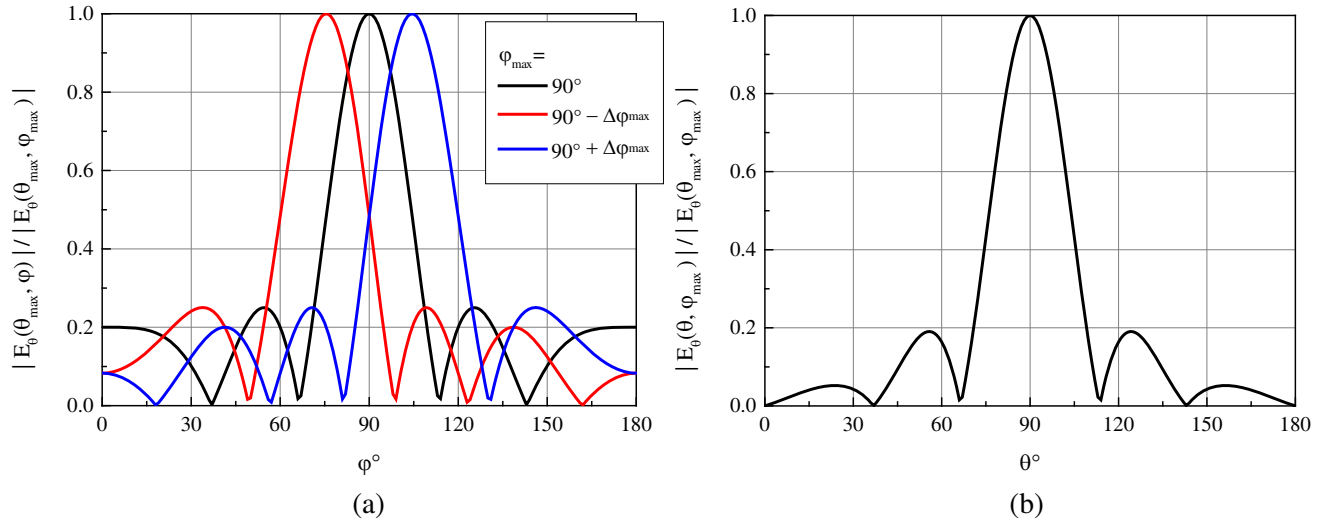


**Figure 2.** The array RPs in the plane  $\theta_{\max} = 90^\circ$  with  $d_z = 0.5\lambda$ ,  $d_x = 0.5\lambda$ , and  $\Delta\varphi_{\max} = 14.4775^\circ$  as functions of: (a) the angle  $\varphi^\circ$ , (b) the angle  $\theta^\circ$ .

Three curves plotted using parameter  $\varphi_{\max}$  equal to  $90^\circ - \Delta\varphi_{\max}$ ,  $90^\circ$ , and  $90^\circ + \Delta\varphi_{\max}$  ( $\Delta\varphi_{\max} = 14.4775^\circ$ ) are shown in Fig. 2(a). The simulation results, that is, the impedance defined by Equation (15) and current arguments in Equation (1) on the vibrators, are presented in Table 1 and Table 2 for angles  $\varphi_{\max} = 104.4775^\circ$  and  $\varphi_{\max} = 75.5225^\circ$ . The row and column indices in the tables,  $n$  and  $m$ , correspond to the positions of the vibrator scatterer in the array structure (Fig. 1).

The simulation data presented in the tables confirm that the absolute value of  $\bar{R}_{nm}$  and  $\bar{X}_{nm}$  are far less than that for active arrays when the vibrators are excited by concentrated electromotive forces [6]. As can be seen, if  $\varphi_{\max} = 75.5225^\circ$ , the negative values  $\bar{R}_{nm}$  and  $\arg(J_{nm})$  are observed simultaneously.

**Table 1.** Simulation results ( $\theta_{\max} = 90^\circ$ ;  $\varphi_{\max} = 104.4775^\circ$ ).

$\bar{R}_{nm}$					$\bar{X}_{nm}$					$\arg(J_{nm}), [^\circ]$				
0	0.0056	0.00792	0.0056	0	0	0.00232	0.00792	0.01352	0.01584	0	45	90	135	180
0	0.0056	0.00792	0.0056	0	0	0.00232	0.00792	0.01352	0.01584	0	45	90	135	180
0	0.0056	0.00792	0.0056	0	0	0.00232	0.00792	0.01352	0.01584	0	45	90	135	180
0	0.0056	0.00792	0.0056	0	0	0.00232	0.00792	0.01352	0.01584	0	45	90	135	180
0	0.0056	0.00792	0.0056	0	0	0.00232	0.00792	0.01352	0.01584	0	45	90	135	180

**Table 2.** Simulation results ( $\theta_{\max} = 90^\circ$ ;  $\varphi_{\max} = 75.5225^\circ$ ).

$\bar{R}_{nm}$					$\bar{X}_{nm}$					$\arg(J_{nm}), [^\circ]$				
0	-0.0056	-0.00792	-0.0056	0	0	0.00232	0.00792	0.01352	0.01584	0	-45	-90	-135	-180
0	-0.0056	-0.00792	-0.0056	0	0	0.00232	0.00792	0.01352	0.01584	0	-45	-90	-135	-180
0	-0.0056	-0.00792	-0.0056	0	0	0.00232	0.00792	0.01352	0.01584	0	-45	-90	-135	-180
0	-0.0056	-0.00792	-0.0056	0	0	0.00232	0.00792	0.01352	0.01584	0	-45	-90	-135	-180
0	-0.0056	-0.00792	-0.0056	0	0	0.00232	0.00792	0.01352	0.01584	0	-45	-90	-135	-180

Thus, the physically correct values of the impedance  $\bar{R}_{nm}$  satisfying the conditions  $\bar{R}_{nm} \geq 0$  can be obtained by changing in Equation (6) the direction of the vibrator's currents on the opposite ones. Since the proposed diffraction antenna array has no elements to control the vibrator currents, this requirement cannot be fulfilled. In other words, if the vibrator array is interpreted from a functional point of view as a thin dielectric layer with effective material parameters, the interval of refraction angles of the incident field satisfying the condition  $\bar{R}_{nm} \geq 0$  determines the refraction angle zone for the material layer, while the interval of angles corresponding to  $\bar{R}_{nm} < 0$  defines an anomalous beam deflection observed, for example, for metamaterials [10, 11].

We have found that the positive values of  $\bar{R}_{nm}$  are observed if the realizable phase difference between the currents on the edge vibrator elements does not exceed  $180^\circ$ . The maximal angle by which the RP can deviate from the normal is defined by the formula

$$\Delta\varphi_{\max} = \arcsin\left(\frac{\pi}{kd_x(N_x - 1)}\right) = \arcsin\left(\frac{\lambda}{2d_x(N_x - 1)}\right) \quad (17)$$

or  $\Delta\varphi_{\max} \approx \frac{\lambda}{2d_x(N_x - 1)} \cdot \frac{180^\circ}{\pi}$  if the deviations are small. If we compare the value of  $\Delta\varphi_{\max}$  defined by Equation (17) with the width of the array RP at the half power level  $\Delta\varphi_{0.5} \approx \frac{\lambda}{d_x(N_x - 1)} \cdot 51^\circ$ , the theoretical level of the maximum deviations is  $\Delta\varphi_{\max} \approx \pm 0.56 \cdot \Delta\varphi_{0.5}$ .

If angle  $\varphi_{\max} = 90^\circ$ , the condition (17) is transformed to

$$\Delta\theta_{\max} = \arcsin\left(\frac{\lambda}{2d_z(N_z - 1)}\right). \quad (18)$$

In this case, the theoretical estimate  $\Delta\theta_{\max} \approx \pm 0.56 \cdot \Delta\theta_{0.5}$  is also valid.

Similar conclusions can be made by analyzing plots of the normalized array RPs defined by Equation (16) if the maxima are deviated in the plane  $\varphi_{\max} = 90^\circ$ . The plots are shown in Fig. 3.

The cross sections of the normalized array RPs as functions of the angular coordinate  $\varphi^\circ$  and  $\theta^\circ$  are plotted in Fig. 3(a) and Fig. 3(b). Three curves corresponding to parameter  $\theta_{\max}$  equal to  $90^\circ - \Delta\theta_{\max}$ ,  $90^\circ$ , and  $90^\circ + \Delta\theta_{\max}$  ( $\theta_{\max} = 14.4775^\circ$ ) are shown in Fig. 3(b). The simulation results are presented in Table 3 and Table 4 for angles  $\theta_{\max} = 104.4775^\circ$  and  $\theta_{\max} = 75.5225^\circ$ .

It is quite clear that the RP maximum of the proposed diffraction antenna array can be scanned in any predefined directions including those lying in diagonal planes by means of varying the impedance  $\bar{R}_{nm}$  of all vibrators. To confirm this conclusion, the main sections of the normalized RP obtained under

**Table 3.** Simulation results obtained for  $\varphi_{\max} = 90^\circ$ ,  $\theta_{\max} = 104.4775^\circ$ .

$\bar{R}_{nm}$					$\bar{X}_{nm}$					$\arg(J_{nm}), [^\circ]$				
0	0	0	0	0	0	0	0	0	0	-180	-180	-180	-180	-180
0.0056	0.0056	0.0056	0.0056	0.0056	0.00232	0.00232	0.00232	0.00232	0.00232	-135	-135	-135	-135	-135
0.00792	0.00792	0.00792	0.00792	0.00792	0.00792	0.00792	0.00792	0.00792	0.00792	-90	-90	-90	-90	-90
0.0056	0.0056	0.0056	0.0056	0.0056	0.01352	0.01352	0.01352	0.01352	0.01352	-45	-45	-45	-45	-45
0	0	0	0	0	0.01584	0.01584	0.01584	0.01584	0.01584	-0	-0	-0	-0	-0

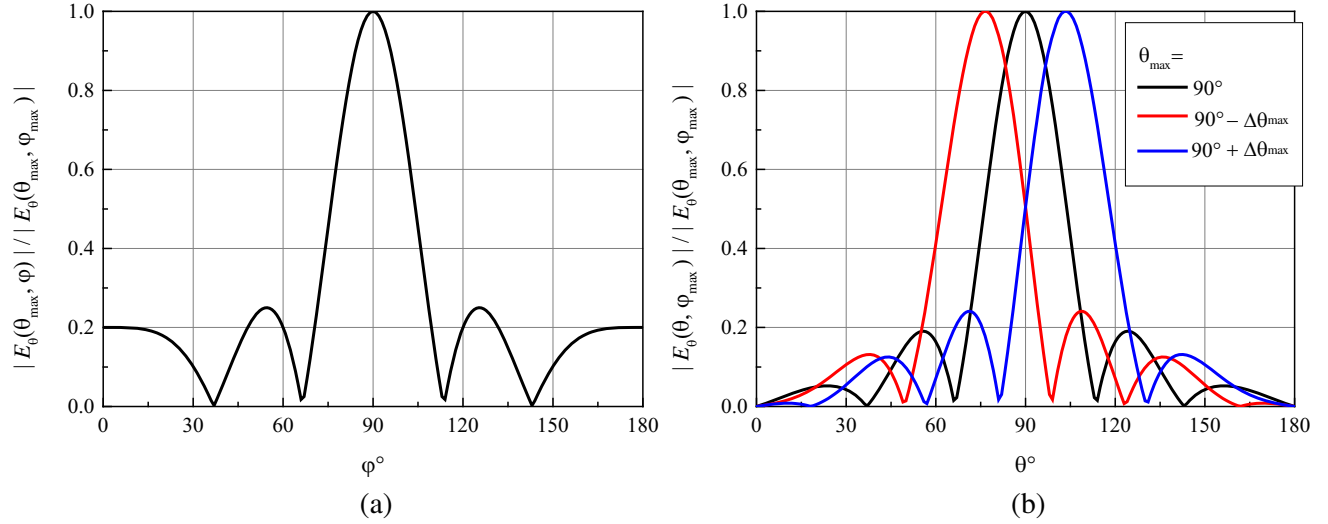


**Figure 3.** The array RPs with  $d_z = 0.5\lambda$ ,  $d_x = 0.5\lambda$ ,  $\varphi_{\max} = 90^\circ$ ,  $\Delta\theta_{\max} = 14.4775^\circ$  as functions of: (a) the angle  $\varphi^\circ$ , (b) the angle  $\theta^\circ$ .

**Table 4.** Simulation results obtained for  $\varphi_{\max} = 90^\circ$ ,  $\theta_{\max} = 75.5225^\circ$ .

$\bar{R}_{nm}$					$\bar{X}_{nm}$					$\arg(J_{nm})$ , $^\circ$				
0	0	0	0	0	0	0	0	0	0	0	0	0	0	0
-0.0056	-0.0056	-0.0056	-0.0056	-0.0056	0.00232	0.00232	0.00232	0.00232	0.00232	-45	-45	-45	-45	-45
-0.00792	-0.00792	-0.00792	-0.00792	-0.00792	0.00792	0.00792	0.00792	0.00792	0.00792	-90	-90	-90	-90	-90
-0.0056	-0.0056	-0.0056	-0.0056	-0.0056	0.01352	0.01352	0.01352	0.01352	0.01352	-135	-135	-135	-135	-135
-0	-0	-0	-0	-0	0.01584	0.01584	0.01584	0.01584	0.01584	-180	-180	-180	-180	-180

the condition  $\varphi_{\max} = \theta_{\max}$  are shown in Fig. 4. We will not present here the corresponding table of the impedances, but we simply indicate that the angular zone of the natural array refraction is within the intervals  $90^\circ \leq \varphi_{\max}, \theta_{\max} \leq 97^\circ$ .

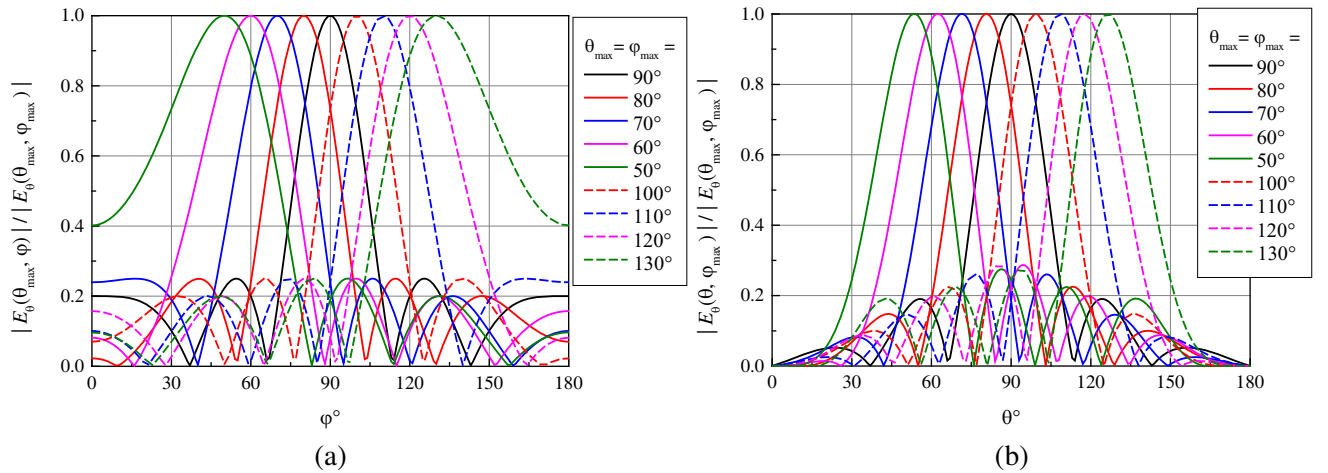


**Figure 4.** The array RPs with  $d_z = 0.5\lambda$ ,  $d_x = 0.5\lambda$ ,  $\varphi_{\max} = \theta_{\max}$  as functions of: (a) the angle  $\varphi^\circ$ , (b) the angle  $\theta^\circ$ .

The relations in Eq. (17) allows us to state that the smaller is the ratio  $d_x/\lambda$ , the wider is the angular zone of natural refraction of the diffraction array in the plane  $\theta_{\max} = 90^\circ$ . As parameter  $d_x/\lambda$  is decreased while  $d_z/\lambda$  is constant (Fig. 1), the array RP gets more pronounced rectangular shape asymmetrically extended in the plane of the smaller side of the diffraction apertures. The plots of the normalized cross sections of the array RP with parameters  $d_z = 0.5\lambda$  and  $d_x = 0.25\lambda$  as functions of the angular coordinate  $\varphi^\circ$  and  $\theta^\circ$  are shown in Fig. 5(a) and Fig. 5(b). Three curves plotted for parameter  $\varphi_{\max}$  equal to  $60^\circ$ ,  $90^\circ$ , and  $120^\circ$  are shown in Fig. 5(a). The simulation results for angles  $\varphi_{\max} = 120^\circ$  and  $\varphi_{\max} = 120^\circ$  are also presented in Table 5 and Table 6.

In this case, the simulation results have shown that the real part of impedance  $\bar{Z}_{nm}$  is always positive if angle  $\theta_{\max} = 90^\circ$ , while angle  $\varphi_{\max}$  varies at interval  $\varphi_{\max} \in [90^\circ, 120^\circ]$ . When the direction

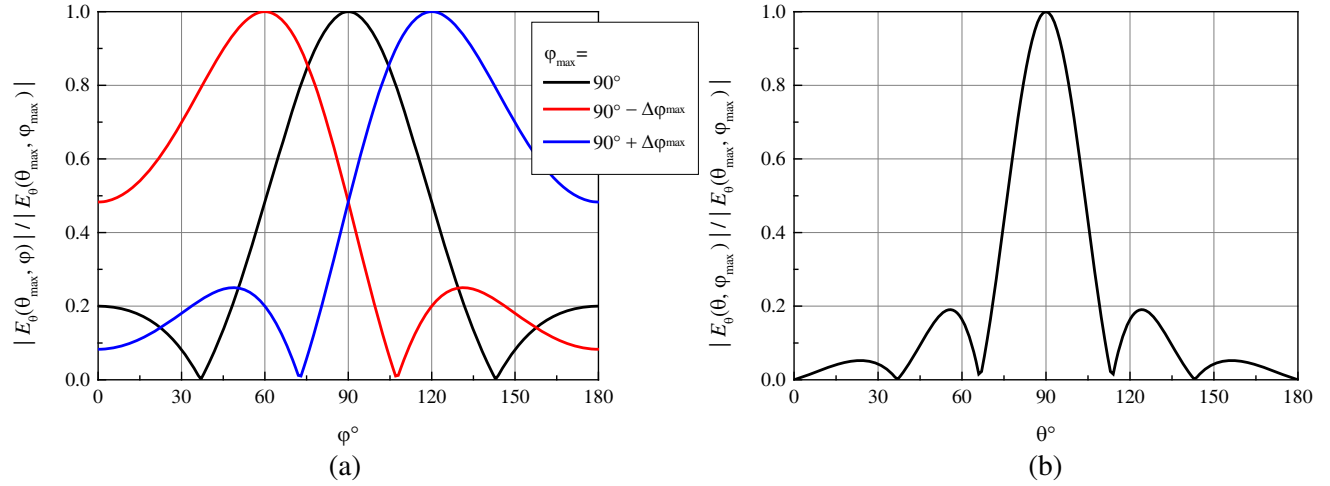


**Figure 5.** The array RPs with  $d_z = 0.5\lambda$ ,  $d_x = 0.25\lambda$ , and  $\theta_{\max} = 90^\circ$  as functions of: (a) the angle  $\varphi^\circ$ , (b) the angle  $\theta^\circ$ .

**Table 5.** Simulation results obtained for  $(\varphi_{\max} = 120^\circ; \theta_{\max} = 90^\circ)$ .

$\bar{R}_{nm}$					$\bar{X}_{nm}$					$\arg(J_{nm}), [^\circ]$				
0	0.0056	0.00792	0.0056	0	0	0.00232	0.00792	0.01352	0.01584	0	45	90	135	180
0	0.0056	0.00792	0.0056	0	0	0.00232	0.00792	0.01352	0.01584	0	45	90	135	180
0	0.0056	0.00792	0.0056	0	0	0.00232	0.00792	0.01352	0.01584	0	45	90	135	180
0	0.0056	0.00792	0.0056	0	0	0.00232	0.00792	0.01352	0.01584	0	45	90	135	180
0	0.0056	0.00792	0.0056	0	0	0.00232	0.00792	0.01352	0.01584	0	45	90	135	180

**Table 6.** Simulation results obtained for  $(\varphi_{\max} = 60^\circ; \theta_{\max} = 90^\circ)$ .

$\bar{R}_{nm}$					$\bar{X}_{nm}$					$\arg(J_{nm}), [^\circ]$				
0	-0.0056	-0.00792	-0.0056	0	0	0.00232	0.00792	0.01352	0.01584	0	-45	-90	-135	-180
0	-0.0056	-0.00792	-0.0056	0	0	0.00232	0.00792	0.01352	0.01584	0	-45	-90	-135	-180
0	-0.0056	-0.00792	-0.0056	0	0	0.00232	0.00792	0.01352	0.01584	0	-45	-90	-135	-180
0	-0.0056	-0.00792	-0.0056	0	0	0.00232	0.00792	0.01352	0.01584	0	-45	-90	-135	-180
0	-0.0056	-0.00792	-0.0056	0	0	0.00232	0.00792	0.01352	0.01584	0	-45	-90	-135	-180

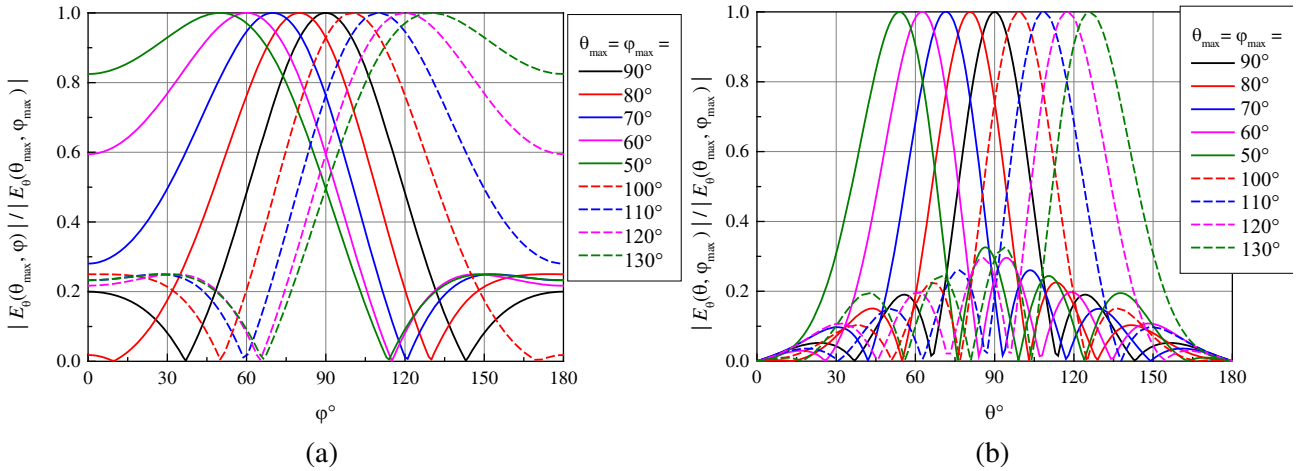


**Figure 6.** The array RPs with  $d_z = 0.5\lambda$ ,  $d_x = 0.25\lambda$ , and  $\varphi_{\max} = \theta_{\max}$  as functions of: (a) the angle  $\varphi^\circ$ , (b) the angle  $\theta^\circ$ .

of the RP maximum varies in the plane  $\varphi_{\max} = 90^\circ$ , the effects similar to those shown in Fig. 3(b) are observed, that is, the angular zone of natural refraction of the diffraction array is  $90^\circ \leq \theta_{\max} \leq 97^\circ$ . The plots of the main sections of the normalized RPs obtained under the condition  $\varphi_{\max} = \theta_{\max}$  are shown in Fig. 6. The simulation results confirm that the sector of the angular zone of the natural refraction for the array is in the range  $(90^\circ \leq \varphi_{\max} \leq 120^\circ; 90^\circ \leq \theta_{\max} \leq 97^\circ)$ .

## 5. CONCLUSION

A new method of impedance synthesis of the antenna array RP proposed earlier by the authors in [6] for a linear array of symmetrical vibrators excited by concentrated voltage generators is generalized for plane 2D diffraction arrays. The problem of impedance synthesis for an antenna array with double periodicity is solved analytically under the condition of unilateral excitation by a plane wave incident along the array normal. Formulas allowing direct calculation of the impedance value on each vibrator are obtained which afford ground for steering the array secondary radiation maximum in a given direction. These formulas can form the basis for the control algorithms of the scattering of diffraction antenna array that are required in practice, for example, for the RD scanning.

Simulation of the antenna array consisting of twenty-five symmetric half-wave vibrators ( $N = 25$ ,  $N_x = 5$ ,  $N_z = 5$ ,  $L = \lambda/4$ ) have confirmed the possibility of the RP beam scanning in front half-space by varying the complex impedances of the vibrators. The physical realizability to ensure that the condition  $\bar{R}_{nm} \geq 0$  holds is analyzed. The limits of the angular zones of natural refraction are defined for the diffraction array with periods ( $d_z = 0.5\lambda$ ;  $d_x = 0.5\lambda$ ) and ( $d_z = 0.5\lambda$ ;  $d_x = 0.25\lambda$ ). Taking into account the reciprocity principle valid for all antenna structures without nonlinear elements, we may state that the results obtained in the work can be used to simulate feed-through diffraction arrays which transform obliquely incident electromagnetic fields into a plane wave propagating in the direction to the array normal.

## REFERENCES

1. Bakhraph, L. D. and S. D. Kremenetskiy, *Synthesis of Radiating Systems (Theory and Methods of Design)*, Sov. Radio, Moscow, 1974 (in Russian).
2. *Microwave Devices and Antennas. Designing Phased Antenna Arrays*, Tutorial/edited by Voskresensky, D. I., Radiotekhnika, Moscow, 2003 (in Russian).
3. Vendik, O. G. and M. D. Parnes, *Antennas with Electric Scanning (Introduction into the Theory)*, Sov. Radio, Moscow, 2001 (in Russian).

4. Berdnik, S. V., V. A. Katrich, M. V. Nesterenko, and Y. M. Penkin, "Electromagnetic waves radiation by a vibrators system with variable surface impedance," *Progress In Electromagnetics Research M*, Vol. 51, 157–163, 2016.
5. Nesterenko, M. V., V. A. Katrich, Y. M. Penkin, V. M. Dakhov, and S. L. Berdnik, *Thin Impedance Vibrators. Theory and Applications*, Springer Science+Business Media, New York, 2011.
6. Penkin, Y. M., V. A. Katrich, and M. V. Nesterenko, "Formation of radiation fields of linear vibrator arrays by using impedance synthesis," *Progress In Electromagnetics Research M*, Vol. 57, 1–10, 2017.
7. Eisenberg, G. Z., *Shortwave Antennas*, Radio i Svyaz', Moscow, 1985 (in Russian).
8. Amitay, N., V. Galindo, and C. P. Wu, *Theory and Analysis of Phased Array Antennas*, John Wiley & Sons Inc, New York, 1972.
9. Lee, R. and S. W. Mittra, *Analytical Techniques in the Theory of Guided Waves*, Macmillan series in electrical science, New York, 1972.
10. Penkin, Y. M., V. A. Katrich, and M. V. Nesterenko, "Impedance synthesis of 2D antenna arrays of slotted spherical radiators," *Progress In Electromagnetics Research Letters*, Vol. 81, 93–100, 2019.
11. Lagarkov, A. N., V. N. Semenenko, A. A. Basharin, and N. P. Balabukha, "Abnormal radiation pattern of metamaterial waveguide," *PIERS Online*, Vol. 4, 641–644, 2008.